Effect of schistosomiasis on CX3CR1-expressing mononuclear phagocytes in the ileum and mesenteric lymph nodes of the mouse

Neurogastroenterology & Motility

Neurogastroenterol Motil (2015) doi: 10.1111/nmo.12658

Effect of schistosomiasis on CX3CR1-expressing mononuclear phagocytes in the ileum and mesenteric lymph nodes of the mouse

K. ALPAERTS,*,# R. BUCKINX,*,# N. COOLS,† M. HEYLEN,‡ S. NULLENS,‡ Z. BERNEMAN,†,§ B. DE WINTER,‡ D. ADRIAENSEN,* L. VAN NASSAUW¶ & J.-P. TIMMERMANS*

*Laboratory of Cell Biology and Histology, Department of Veterinary Sciences, University of Antwerp, Antwerp, Belgium
†Laboratory of Experimental Hematology, Vaccine and Infectious Disease Institute (Vaxinfectio), Faculty of Medicine and Health Sciences, University of Antwerp, Antwerp University Hospital (UZA), Edegem, Belgium
‡Laboratory of Experimental Medicine and Pediatrics, Faculty of Medicine and Health Sciences, University of Antwerp, Antwerp, Belgium
§Center for Cell Therapy and Regenerative Medicine, Antwerp University Hospital (UZA), Edegem, Belgium
¶Laboratory of Human Anatomy and Embryology, Faculty of Medicine and Health Sciences, University of Antwerp, Antwerp, Belgium

Key Messages

- The results presented in this study demonstrate the importance of the CX3CR1-expressing DC and MΦ subsets in intestinal immune surveillance and in the immune response against parasitic infection.
- The aim of this study was to investigate the effect of *Schistosoma mansoni*-induced inflammation on the distribution of the different mononuclear phagocyte (MNP) populations in the ileum and MLNs of the mouse. In addition, the uptake and processing of schistosomal antigens by different MNPs in the LP and MLNs were studied *in situ* at different time points to determine which, and to what extent, DC or MΦ subsets are involved.
- We used a combined strategy of immunohistochemistry, confocal microscopy and multiparametric flow cytometry. For quantitative analysis, ImageJ software (public domain, NIH) and Volocity software (PerkinElmer Inc., Waltham, MA, USA) were used. FlowJo software was applied to analyze the multiparametric flow cytometry data.
- We demonstrated a significant upregulation of the CD11c$^+$ CX3CR1$^+$ F4/80$^-$ DCs during *S. mansoni*-induced inflammation both in the ileum and in the MLNs indicating the involvement of this subset in helminth infections. In addition, we showed that all CX3CR1-expressing MNPs are responsible for a swift uptake and processing of parasitic antigens.

Abstract

Background *Intestinal dendritic cells (DCs) maintain immune homeostasis, only initiating an active immune response against invading pathogens. However, little information is available on the reaction of mononuclear phagocytes (MNP) to intestinal trematode infection, a reaction equally important in helminth-based therapies. The CD11c$^+$ CX3CR1$^+$ F4/80$^-$ DCs in the ileal lamina propria (LP) of the mouse were proven to migrate to the mesenteric lymph nodes (MLNs). We analyzed all MNP subsets present in the mouse LP and MLNs, under steady-state conditions and during acute Schistosoma mansoni-induced inflammation. Furthermore, we studied the uptake of schistosomal antigens by MNP in vivo in the LP and*

Address for Correspondence
Prof. Dr. Jean-Pierre Timmermans, University of Antwerp, Groenenborgercampus, Groenenborgerlaan 171, 2020 Antwerp, Belgium.
Tel: +3232653327; fax: +3232653301;
e-mail: jean-pierre.timmermans@uantwerpen.be
#The first two authors contributed equally to the manuscript.
Received: 16 May 2015
Accepted for publication: 22 July 2015

MLNs. ***Methods*** *Using a combination of immunohistochemistry and multiparametric flow cytometry, we investigated distributional changes of the MNP during acute intestinal schistosomiasis. Next, S. mansoni-derived products, i.e., S. mansoni soluble worm proteins (SmSWP) and S. mansoni soluble egg antigens (SmSEA) were intraperitoneally injected into CX3CR1$^{+/GFP}$ C57BL/6 mice and antigen uptake was analyzed using confocal microscopy.* ***Key Results*** *The CD11c^{+} CX3CR1^{+} F4/80^{-} DCs significantly increased during intestinal schistosomiasis in the LP and MLNs. Only CX3CR1-expressing DC and MΦ subsets, but not other LP DCs, are involved in both SmSWP and SmSEA antigen uptake and processing.* ***Conclusions & inferences*** *The significant upregulation of CD11c^{+} CX3CR1^{+} F4/80^{-} DCs during intestinal schistosomiasis and the restriction of phagocytosis of parasitic antigens to CX3CR1-expresssing MNP indicate a crucial role for this immune cell niche in response to trematodiasis. These findings add insight into the functional specialization of LP immune cells and add to the understanding of cellular mechanisms behind helminth-based therapies.*

Keywords *antigen uptake, dendritic cells, intestinal schistosomiasis, macrophages.*

INTRODUCTION

The gastrointestinal (GI) tract is continuously exposed to a myriad of antigens, ranging from harmless organisms to potentially invading pathogens, necessitating a delicate equilibrium between preserving immune homeostasis and mounting an active immune response. Dendritic cells (DCs) are imperative in the regulation and maintenance of the balance between immunity *vs* tolerance.[1] In the intestine, DCs uphold immune homeostasis and trigger an appropriate immune response only when needed.[2] Disturbance of this balance initiates an overactive immune response, potentially leading to GI disorders, such as inflammatory bowel disease (IBD).[3]

Lamina propria (LP) DCs express CD11c and major histocompatibility complex class II molecules[4,5] and are subclassified into two subgroups using CD103 (integrin αE) or CX3CR1 (fractalkine receptor).[6] The absence of F4/80 or CD64 expression distinguishes them from macrophages (MΦ).[7,8] Both subsets have a different ontogeny.[9,10]

Only CD103^{+} LP DCs were presumed to migrate to the mesenteric lymph nodes (MLNs)[8,11] although recently it was proven that CX3CR1^{+} cells are also migratory.[12,13] The exact function of this CD11c^{high}CX3CR1^{intermediate}F4/80^{-} DC subset is largely unknown. The CX3CR1^{+} cells continuously sample the intestinal lumen[14] and fenestrated capillaries,[15] pointing to a role of CX3CR1^{+} cells in intestinal and circulatory immune surveillance. Further detailed information about the two main LP DC subsets in the ileum of the mouse can be found in two recent reviews.[16,17] Currently, knowledge on the distribution of the LP DCs during parasitic intestinal inflammation or how this affects the DCs in the MLNs is still lacking.

Schistosomiasis is a parasitic disease caused by a blood trematode of the *Schistosoma* genus, where eggs cause extensive granuloma formation and inflammation in the liver and intestine.[18] The acute phase of *S. mansoni*-induced inflammation in the mouse model is characterized by a T helper 1 (Th1)-type immune response which develops into a Th2-type immune response directed against the egg antigens, e.g., omega-1, when oviposition starts.[19–22] *Schistosoma mansoni*-derived soluble worm proteins (SmSWP) or egg antigens (SmSEA) are immunomodulatory, inducing a Th2 response, anergy or an inhibition of a deleterious Th17 immune response.[23–25] To date, information about the effects of trematode-induced inflammation on the DC or MΦ distribution in these organ systems remains elusive. Given the long tradition of working with *S. mansoni*-induced ileal inflammation in our laboratory,[18,26,27] and the fact that the majority of immunological research is focused on the DC and MΦ subsets in the mouse ileum,[28] the research presented in this study will focus on the ileum as the region of interest.

The aim of this study was to investigate the effect of *S. mansoni*-induced inflammation on the distribution of the different mononuclear phagocyte (MNP) populations in the ileum and MLNs of the mouse using a combined approach of immunohistochemistry (IHC), confocal microscopy and multiparametric flow cytometry (MPFC). In addition, the uptake and processing of schistosomal antigens by different MNPs in the LP and MLNs were studied *in situ* at different time points to determine which, and to what extent, DC or MΦ subsets are involved.

MATERIALS AND METHODS

Tissue preparation

Animal housing and handling procedures were conducted in accordance with the European directive 86/609/EEC. All experiments were approved by the Ethical Commission of the University of Antwerp, Belgium. Heterozygous male CX3CR1$^{+/GFP}$

C57BL/6 mice, 8 weeks old, were intraperitoneally (i.p.) infected with a Puerto Rican strain of *S. mansoni* following an adapted procedure of Yolles *et al.*[29] Animals were sacrificed 8 weeks post infection (wpi). CX3CR1$^{+/GFP}$ C57BL/6 mice were kindly provided by Prof. P. Ponsaerts (Experimental Cell Transplantation Group, Laboratory of Experimental Hematology, Vaccine and Infectious Disease Institute [Vaxinfectio], University of Antwerp, Antwerp, Belgium) and originally created by Jung *et al.*[30] The animals were housed in a 12 h light/12 h dark cycle at a constant ambient temperature of 22 °C and had *ad libitum* access to water and standard pellet food. Animals were euthanized at the age of 16 weeks by cervical dislocation followed by exsanguination. The ileum and the MLNs were excised and immediately washed in cold physiological Krebs solution (117 mM NaCl, 5 mM KCl, 2.5 mM $CaCl_2{\cdot}2H_2O$, 1.2 mM $MgSO_4{\cdot}7H_2O$, 25 mM $NaHCO_3$, 1.2 mM $NaH_2PO_4{\cdot}2H_2O$, and 10 mM glucose at pH 7.4). Tissues for IHC were fixed in Zamboni's fixative, washed in 0.01 M PBS (pH 7.4) and further processed to optimize the immunocytochemical staining as previously described.[31] Subsequently, the tissues were incubated overnight at 4 °C in 30% sucrose before being embedded in OCT (Pelko Int., Torrance, CA, USA), sectioned in a cryostat at 12 μm and thaw-mounted on poly-L-lysine-coated slides, which were stored at −20 °C. Tissues for flow cytometric analysis underwent a specific dissociation- and isolation protocol as described below.

Tissue dissociation and isolation protocol

After being rinsed in Krebs solution, ileal tissue was cut into small pieces of approximately 0.5 cm, incubated in Dispase II (Roche Diagnostics, Basel, Switzerland) at 37 °C for 90 min and subsequently incubated in Collagenase A (Roche Diagnostics) for 120 min at 37 °C. Next, the tissue homogenate was mechanically dissociated using a 19G needle until a single cell suspension was obtained. The MLNs were excised and immediately placed in cold RPMI 1640 medium (Life Technologies Europe B.V., Ghent, Belgium) and dissociated mechanically using a 40 μm nylon cell strainer (BD Biosciences, San Jose, CA, USA) as previously described by Ruyssers *et al.*[32] The obtained single cell suspension was rinsed in RPMI 1640 medium. Following centrifugation, the cell pellet was suspended in red blood cell lysis buffer (Sigma Aldrich, Buchs, Switzerland). Subsequently, the cells were washed and the cell pellet was suspended in RPMI 1640 medium. Debris was removed by transferring the cells in medium over a 40 μm nylon cell strainer. Next, the single cell suspension was stained for flow cytometric analysis.

Multiparametric flow cytometry

Analyses were performed in accordance with the recommended guidelines for reliable and reproducible MPFC experiments as previously described.[33,34] After single cell suspensions for ileum (non-infected animals, $n = 5$ and *S. mansoni*-infected animals, $n = 5$) and MLNs (non-infected, $n = 10$ and *S. mansoni*-infected animals, $n = 11$) had been obtained, the cells were incubated for 15 min at 4 °C with different anti-mouse antibodies (Table S1). The 'Fluorescence Minus One' (FMO) method was used as a control for determining the correct gate settings.[34–36] Cell viability was tested and yielded 91.77% ± 1.48% viable cells (mean ± SEM; Invitrogen's live/dead cell viability assay, Carlsbad, CA, USA). Next, cells were washed and analyzed on a FACSAria II (BD Biosciences). The gating strategies employed for ileum (Fig. S1) and MLNs (non-infected and *S. mansoni*-infected; Fig. S2) are enclosed. Necessary compensation settings were included. For the MLN analysis, the stopping gate was set at 50 000 total events FSC/SSC identified. For the ileum, the whole sample was measured without a stopping gate. The results were analyzed using FlowJo (v9.5.3 FlowJo LLC., Ashland, OR, USA) and statistical analysis was performed using an unpaired Student's *t*-test (tail 2, type 2) with *p*-values of ≤0.05 considered as statistically significant.

Immunohistochemistry

All immunohistochemical staining procedures were carried out at room temperature and performed on 12 μm thick cryosections of non-infected and *S. mansoni*-infected ileum and MLNs of CX3CR1$^{+/GFP}$ C57BL/6 mice including the animals that received an i.p. injection of SmSWP and SmSEA. Unless indicated otherwise, washing steps were carried out with 0.01 M PBS. After rinsing the cryosections first, non-specific avidin-binding activity and avidin binding to endogenous biotin was blocked using an avidin/biotin blocking kit (Life Technologies Europe B.V.) as previously described.[37] Next, the cryosections were immersed for 2 h in 0.01 M PBS containing 10% normal horse serum (NHS), 0.05% thimerosal and 1% Triton X-100 prior to incubation for 16 h with an primary antibody raised against mouse CD11c, CD103, F4/80 or LAMP-1 (Table S2) diluted in 0.01 M PBS containing 10% NHS, 0.05% thimerosal and 0.1% Triton X-100. The crysections were then incubated for 1 h with the corresponding biotinylated secondary antibodies (Table S2) diluted in the same solution. Visualization was performed using a fluorophore-conjugated streptavidin diluted in 0.01 M PBS for 2 h. Finally, cryosections were mounted in Citifluor (Citifluor Ltd., London, UK). For each immunolabeling, immunolabelings with corresponding isotype control antibodies (Table S2) and negative controls in which the primary antibody was omitted were performed. The labeled cryosections were evaluated using either fluorescence microscopy (Zeiss Axiophot, Oberkochen, Germany) or confocal microscopy (UltraView Vox; PerkinElmer Inc., Waltham, MA, USA).

Quantitative analysis of MNP subtypes

Quantitative analysis of the images made with fluorescence microscopy and confocal microscopy was performed using ImageJ software (public domain, NIH) and Volocity software (PerkinElmer Inc.), respectively. For each marker, immunopositive cells were counted in 15 randomly selected villi from three non-consecutive cryosections in each animal. Three different animals per condition (control *vs* intestinal schistosomiasis) were used. The area of interest was determined by marking the entire villus surface up to the muscularis mucosae. The results, expressed as means ± SEM, were analyzed using an unpaired Student's *t*-test (tail 2, type 2) with *p*-values of ≤0.05 considered statistically significant. Exact *p*-values are mentioned in the results section.

Uptake of helminth soluble fractions

Healthy CX3CR1$^{+/GFP}$ C57BL/6 mice were i.p. injected with SmSWP or SmSEA. Experiments were carried out *in duplo*. The SmSWP were prepared as described previously by our groups.[32,38] Briefly, at 8 wpi, adult worms were collected by portal venous perfusion, washed in PBS, homogenized with a glass tissue grinder and centrifuged, giving rise to the soluble fraction. The total protein concentration was established using the rapid protein-selective colorimetric Bradford method following the manufac-

turer's instructions (Coomassie Plus, The Better Bradford Assay kit; Thermo Scientific Inc., Waltham, MA, USA). The SmSWP were stored at −80 °C. The SmSEA, a kind donation of Dr. G. Schramm (Research Center Borstel, Borstel, Germany), were prepared with slight modifications.[39] Briefly, the eggs were collected from the livers of *S. mansoni*-infected mice. After tissue homogenization, eggs were separated from the tissue by using sieves, placed in PBS and washed 10 times by centrifugation with PBS. Subsequently, the eggs were homogenized with a glass homogenizer and after centrifugation; the soluble fraction was obtained and stored at −80 °C. Total protein concentration was ascertained by employing the MicroBCA-Kit (Thermo Scientific Inc.) and endotoxin levels were determined with the LAL-Haemochrom-Assay (Cape Cod Inc., East Falmouth, MA, USA). The SmSWP and SmSEA fractions were fluorescently linked with the Chromeo™P543 labeling kit (Active Motif Inc., Carlsbad, CA, USA), following the manufacturer's guidelines, and injected i.p. at a final concentration of 25 μg.[25,32] The animals treated with SmSEA were sacrificed 1 h and 18 h after SmSEA injection in line with the study of Chang *et al.*[15] The same time points were selected for the SmSWP experiments and additional time points were added to further determine the exact time when SmSWP are captured by the MNPs in the ileum and MLNs. Negative controls were performed by i.p. injection of mice with the diluted Chromeo P543™ fluorophore in the recommended buffer.

RESULTS

Mononuclear phagocytes in the healthy mouse ileum

The distribution of the DC and MΦ subpopulations in the mouse terminal ileum was investigated under steady-state conditions using flow cytometry. The total leukocyte cell population was identified using CD45 membrane marker expression.[40] Fig. S1A depicts the gating strategy used to obtain the flow cytometry data in Table 1. The CX3CR1$^+$ cell population was further characterized based on the expression of F4/80 or CD11c, resulting in the identification of a CD11c$^+$ CX3CR1$^+$ F4/80$^-$ DC and a CX3CR1$^+$ F4/80$^+$ MΦ subset (Fig. S1B, C and E; Table 1). Our findings demonstrated a comparable number of CX3CR1$^+$ DCs and CX3CR1$^+$ MΦs (34.79 ± 6.25% *vs* 29.38 ± 4.42%, mean ± SEM) in the non-inflamed mouse ileum. The remaining CX3CR1$^+$ cell fraction most likely consisted of monocytes which do not express CD11c or F4/80. The ileum of CX3CR1$^{+/GFP}$ C57BL/6 mice with intestinal schistosomiasis could not be analyzed with MPFC without compromising cell viability. Therefore, IHC and manual counts were performed on cryosections of *S. mansoni*-inflamed ileum and compared to non-inflamed ileum. As such, a complementary IHC and flow cytometry approach was adopted to obtain the aimed information.

Table 1 Flow cytometric quantitative analysis of the healthy ileum

Marker	Mean ± SEM (%)
Control conditions	
CD103	3.30 ± 1.05
CX3CR1	7.22 ± 2.33
CD11c	10.64 ± 1.78
F4/80	4.74 ± 0.67
CD11c$^+$ CX3CR1$^+$	34.79 ± 6.25
F4/80$^+$ CX3CR1$^+$	29.38 ± 4.42

Mean percentages of all mononuclear phagocyte (MNP) populations present in a single cell suspension of ileal cells with corresponding SEM. Percentages of CD11c$^+$ CX3CR1$^+$ cells and F4/80$^+$ CX3CR1$^+$ cells are relative to the general CX3CR1$^+$ cell population. The schistosoma-inflamed ileum could not be analyzed flow cytometrically, since pathological changes prevented obtaining a viable single cell suspension.

Distribution of ileal MNP populations during intestinal schistosomiasis

To gain insight into possible distributional changes in intestinal MNP subsets during *S. mansoni*-induced inflammation, the density of these subpopulations was quantitated using (immune) fluorescence and confocal microscopy. Significantly broadened villi were observed during intestinal schistosomiasis as previously described.[18] As this impacts both the surface area and the density compared to the steady-state conditions, absolute cell numbers within the area of interest were also determined. Although we did not detect any significant differences in the density of the CX3CR1$^+$ cell population (3714 ± 16 *vs* 3671 ± 16 cells/mm^2, $p = 0.894$; Fig. 1A) or in absolute CX3CR1$^+$ cell numbers (429 ± 51 *vs* 564 ± 63 cells/15 villi, $p = 0.179$; Fig. 1B), a significant increase in the absolute cell number of CD11c$^+$ CX3CR1$^+$ F4/80$^-$ DCs was observed during *S. mansoni-induced* inflammation (159 ± 17 *vs* 260 ± 17 cells/15 villi, $p = 0.0135$; Fig. 1D), indicative of a cellular redistribution within the CX3CR1 population during inflammation. As far as the CX3CR1$^+$ F4/80$^+$ MΦ subset is concerned, no differences in density or absolute cell numbers were detected (1292 ± 2 *vs* 992 ± 2 cells/mm^2, $p = 0.097$; 139 ± 10 *vs* 164 ± 23 cells/15 villi, $p = 0.388$; Fig. 1E and F).

Mononuclear phagocyte populations within the MLNs

Subsequently, the distribution of MNPs in the MLNs, particularly the CD11c$^+$ CX3CR1$^+$ F4/80$^-$ DCs, was investigated under steady-state conditions and during *S. mansoni*-induced inflammation. Our results disclosed several significant changes in the distribution of the MNP populations during intestinal schistosomiasis (Table 2; Fig. S3). Firstly, a significant increase in the general CD11c$^+$ and CD11c$^+$ CX3CR1$^+$ cell populations was observed (Table 2; Fig. S4A). Further-

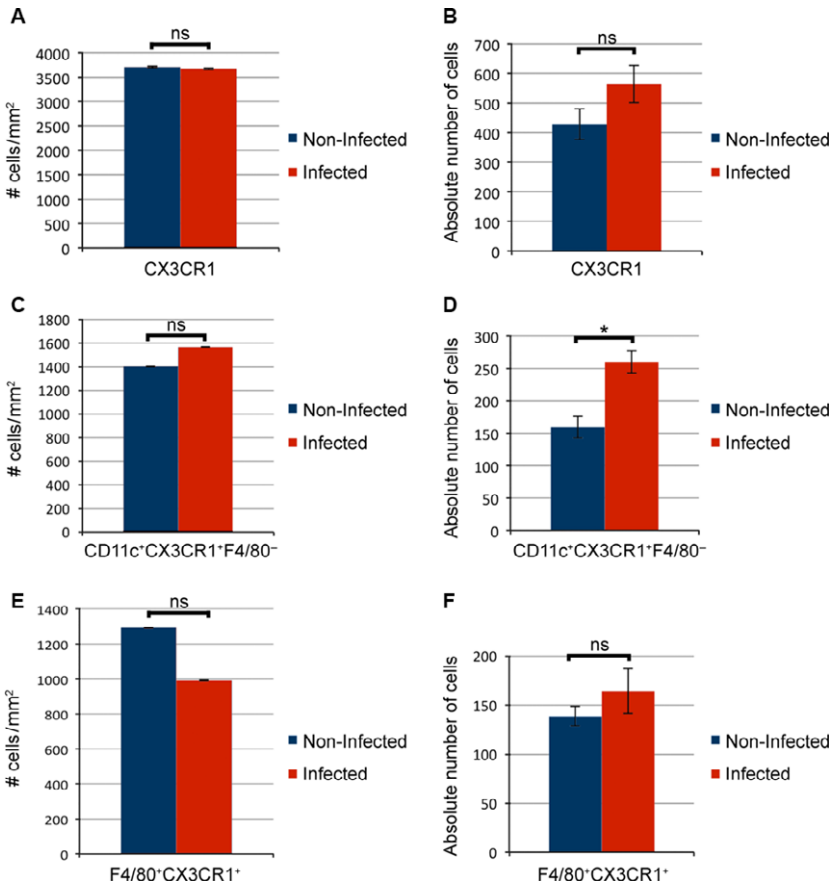

Figure 1 Immunohistochemical quantitative analysis of mononuclear phagocyte (MNP) subtypes in the ileal lamina propria (LP). Immunolabeling of cryostat sections of non-infected ileum (in blue) and *Schistosoma mansoni*-infected ileum (in red) followed by manual cell counts of cells in the LP up to the muscularis mucosae. Analysis with ImageJ and Student's *t*-test where $*p \leq 0.05$ is considered as significant; NS, non-significant. The cell density (number of cells per mm^2) was calculated (A, C and E). Given the significant broadening of the intestinal villi during intestinal schistosomiasis, also the absolute number of cells was counted for the total number of villi that were analyzed (15 villi per animal, $N = 3$) (B, D and F). A significant increase in total $CD11c^+$ $CX3CR1^+$ $F4/80^-$ DC cell numbers was observed during inflammation (D).

Table 2 Flow cytometric quantitative analysis of the MLNs

Marker	Control conditions Mean ± SEM (%)	Intestinal schistosomiasis Mean ± SEM (%)	Statistical analysis	
			Significance	*p*-value
CD103	25.50 ± 1.16	19.70 ± 0.57	**	0.0002
CX3CR1	2.38 ± 0.27	2.37 ± 0.15	NS	0.978
CD11c	3.23 ± 0.21	4.90 ± 0.27	**	0.0001
$CD11c^+$ $CD103^+$	1.17 ± 0.10	2.22 ± 0.19	**	0.0002
$CD11c^+$ $CX3CR1^+$	0.54 ± 0.07	0.77 ± 0.04	*	0.012
$CD11c^+$ $CX3CR1^+$ $F4/80^-$	0.38 ± 0.06	0.63 ± 0.04	**	0.002
F4/80	1.64 ± 0.17	2.66 ± 0.31	*	0.012
$F4/80^+$ $CX3CR1^+$	0.30 ± 0.04	0.31 ± 0.03	NS	0.863
$CD11c^+$ $CX3CR1^+$ $F4/80^+$	0.16 ± 0.02	0.13 ± 0.02	NS	0.244

Mean percentages of all mononuclear phagocyte (MNP) populations present in the mesenteric lymph nodes (MLNs) relative to the general $CD45^+$ leukocyte population under control conditions and during intestinal schistosomiasis with corresponding SEM. Statistical analysis has been carried out using an unpaired Student's *t*-test (tail 2, type 2) with *p*-values of ≤0.05 considered as statistically significant; *significant at $p \leq 0.05$, **significant at $p \leq 0.005$ and NS, non-significant.

more, the $CD11c^+$ $CD103^+$ DC cell population was also significantly expanded, whereas the general $CD103^+$ cell subset was significantly decreased during inflammation (representative dot plots Fig. S3A *vs* I; Table 2). The total $F4/80^+$ cell population was also significantly expanded but no changes in the number of the $CX3CR1^+$ cells were detected during schistosomiasis (Fig. S3D *vs* L, Fig. S3B *vs* J; Table 2). Further analysis of the $CD11c^+$ $CX3CR1^+$ subpopulation revealed that the $CD11c^+$ $CX3CR1^+$ $F4/80^-$ DC proportion within this subpopulation was increased by nearly twofold during inflammation, while no significant

changes were observed for the CD11c$^+$ CX3CR1$^+$ F4/80$^+$ MΦ subset (Fig. S3H *vs* Fig. S3P; Table 2).

Antigen uptake

We investigated the kinetics of antigen uptake by MNPs in the ileum and MLNs at different time points following injection of the mice with either SmSWP or SmSEA, *i.e.*, 2 min, 5 min, 15 min, 30 min, 1 h, and 18 h post injection (p.i.) for the SmSWP and 1 h and 18 h after administration of SmSEA. The micrographs of the ileum clearly show red blood cells (Figs. 2 and 4; Fig. S5) in the red channel. This observation can be 'explained' by a binding of labeled worm proteins to the red blood cell membrane.[41] After analyzing the ileal tissue and MLNs from the mice injected with solely the fluorophore and recommended buffer, red blood cells did not show red fluorescence indicating that no background fluorescence from the conjugated fluorophore was present. Immunostainings performed to detect CD11c and F4/80 in the ileal tissues showed that at 2 min p.i. (Fig. 2C) not all SmSWP antigens were engulfed by MNPs (asterisk, Fig. 2A) although several CX3CR1$^+$ cells contained SmSWP (Fig. 2C and M, arrow). For both antibodies, CD11c and F4/80, corresponding isotype control antibodies showed no staining (Fig. S6). The CD11c$^+$ CX3CR1$^+$ cells (Fig. 2C, arrow) and F4/80$^+$ CX3CR1$^+$ cells (Fig. 2M, open arrow) displaying engulfed SmSWP were clearly present throughout the LP. At 5 min p.i., some free SmSWP could still be detected (Fig. 2D, asterisk) in the LP, while the present CD11c$^-$ CX3CR1$^+$ cells and CD11c$^+$ CX3CR1$^+$ cells (Fig. 2D, arrow) had phagocytized the SmSWP antigens (Fig. 2D). From 15 min p.i. onwards (Fig. 2E–L), all SmSWP were engulfed by different types of MNPs (CX3CR1$^+$ cells and CD11c$^+$ CX3CR1$^+$ DC-like cells) in the LP. At later time points, *i.e.*, 1 h p.i. (Fig. 2N) and 18 h p.i. (Fig. 2O), both F4/80$^+$ CX3CR1$^-$ cells (Fig. 2N, arrow) and F4/80$^+$ CX3CR1$^+$ cells (Fig. 2N, open arrow) with engulfed SmSWP were observed.

At 2 min p.i., almost no antigen-loaded CD11c$^+$ (Fig. 3A) or antigen-loaded F4/80$^+$ (Fig. 3D) cells were detected in the MLNs, whereas the CD11c$^-$ CX3CR1$^+$ (Fig. 3A, arrow) and F4/80$^-$ CX3CR1$^+$ cells (Fig. 3D) showed already engulfed SmSWP antigens. A visible increase in CD11c$^+$ CX3CR1$^-$ and CD11c$^+$ CX3CR1$^+$ cells (Fig. 3B) was observed in the MLNs between 1 h p.i. and 18 h p.i. (Fig. 3C). Both CX3CR1$^+$ cells and CD11c$^+$ CX3CR1$^+$ cells displayed engulfed SmSWP antigens. Accordingly, a visible increase in F4/80$^+$ CX3CR1$^-$ cells and F4/80$^+$ CX3CR1$^+$ MΦs (Fig. 3E), was observed at 1 h p.i. and both cell subsets revealed phagocytized SmSWP antigens. At 18 h p.i. (Fig. 3F), F4/80$^+$ cells and F4/80$^+$ CX3CR1$^+$ MΦ's were still discernable.

Next, SmSEA uptake was investigated to determine whether there were any differences in antigen uptake or processing or whether the MNP subsets showed aberrant behavior after injection of egg antigens only. The SmSEA experiments included two time points and yielded results for the ileum that were similar to the ileal SmSWP assay results. The CD11c and F4/80 immunolabelings of the ileum showed that CD11c$^-$ CX3CR1$^+$ cells, CD11c$^+$ CX3CR1$^+$ DC-like cells, F4/80$^-$ CX3CR1$^+$ cells and F4/80$^+$ CX3CR1$^+$ MΦs had engulfed the SmSEA antigens at 1 h p.i. (Fig. 4C and I) and 18 h p.i. (Fig. 4F and L). The immunolabelings on the MLNs equally showed similar results to those observed with the SmSWP experiments. The CD11c$^+$ CX3CR1$^-$ cells (Fig. 5A), F4/80$^-$ CX3CR1$^+$ cells (Fig. 5C, arrow) and some F4/80$^+$ CX3CR1$^+$ cells were all loaded with SmSEA at 1 h p.i. (Fig. 5C, open arrow). The antigen-loaded CD11c$^+$ CX3CR1$^-$ cells persisted up to 18 h p.i. (Fig. 5B). In addition, at 18 h p.i. (Fig. 5D) antigen-loaded F4/80$^+$ CX3CR1$^-$ cells and F4/80$^+$ CX3CR1$^+$ MΦs were visible in the MLNs. An overview of the anatomical distribution of the immune cells involved in schistosomal antigen uptake is shown in Fig. S7. Cells which have phagocytized the antigens are located predominantly in the medulla.

Finally, we determined the intracellular location of the SmSWP and SmSEA proteins of antigen-loaded MNPs, by performing immunostainings with LAMP-1. Our findings demonstrated that SmSWP (Fig. S5A) and SmSEA (Fig. S5B) were located within the lysosomes.

DISCUSSION

Functional and phenotypical research on intestinal MNPs is important to reveal how the immunological defense mechanisms of the intestinal LP function. In this study, focus was placed on the elaborate network of intestinal LP DCs consisting of several specialized cell subsets. The CX3CR1$^+$ DC subset, *i.e.*, the CD11c$^+$ CX3CR1$^+$ F4/80$^-$ DCs, has gained renewed interest since it was recently discovered that these DCs are not residential as previously thought, but are capable of migration[12,13] and are involved in circulatory and intestinal immune surveillance.[14,15] To our knowledge, our understanding of the function or behavior of this DC subset during intestinal inflammation is largely unexplored. Overall, the effects of helminth-induced inflammation on DCs or MNPs have been poorly investigated. Only one study has reported on a particular DC subset (designated as CD11c^{low} CD103$^-$ DCs) that

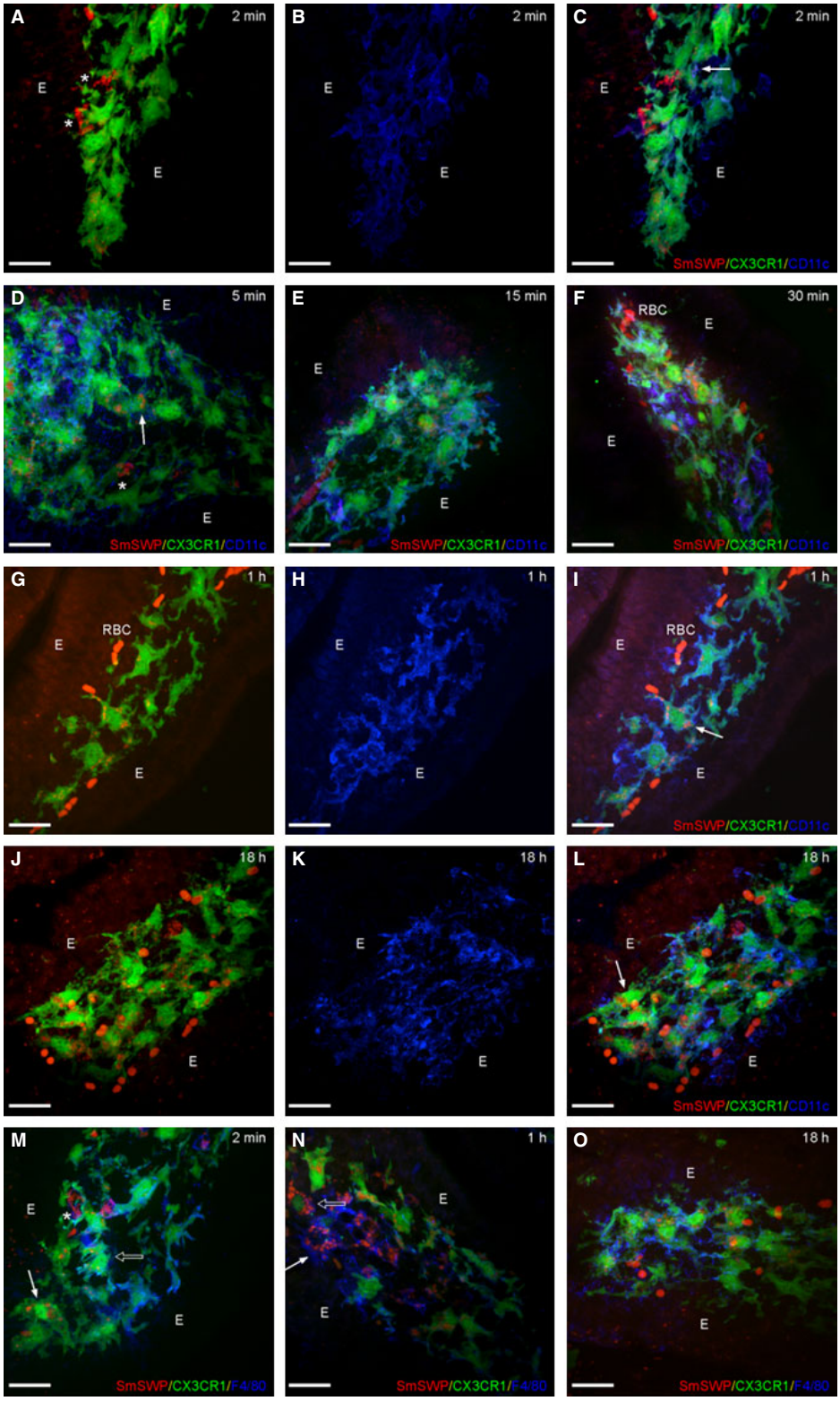

Figure 2 Uptake of SmSWP in the ileal lamina propria (LP). Cryosections of the ileum of CX3CR1$^{+/GFP}$ C57BL/6 mice immunostained for CD11c (A–L, in blue) or F4/80 (M–O, in blue) after *in vivo* SmSWP (in red) injections at different time points. CX3CR1^{+} cells (L and M, arrow), CD11c^{+} CX3CR1^{+} cells (C, arrow; D, arrow; I, arrow), F4/80^{+} cells (N, arrow) and F4/80^{+} CX3CR1^{+} cells (M-N, open arrow). Asterisk (*) indicates unbound SmSWP. E, epithelium; RBC, red blood cells. Scale bar: 20 μm.

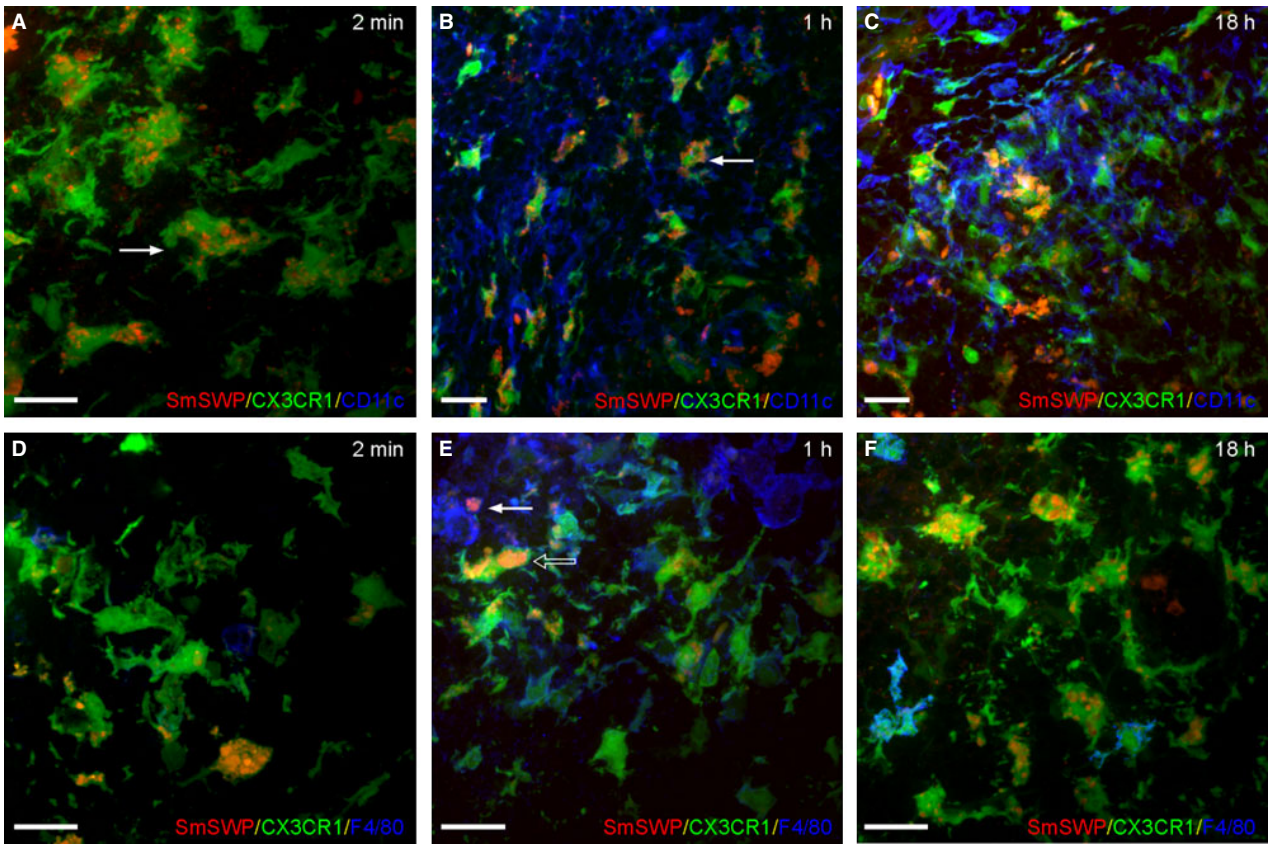

Figure 3 Uptake of SmSWP in the mesenteric lymph nodes (MLNs). Cryosections of the MLNs of CX3CR1$^{+/GFP}$ C57BL/6 mice immunostained for CD11c (A–C) or F4/80 (D–F) after *in vivo* SmSWP injections at different time points. CX3CR1^{+} cells (A, arrow), CD11c^{+} CX3CR1^{+} cells (B, arrow), F4/80^{+} cells (E, arrow) and F4/80^{+} CX3CR1^{+} cells (E, open arrow). Scale bar: 20 μm.

was significantly increased in MLNs during a *Heligmosomoides polygyrus bakeri*-infection.[42] In the present study, possible changes in the ileal CD11c^{+} CX3CR1^{+} F4/80^{-} DC subset under control conditions were studied using flow cytometry. Due to the rigidity of the ileum, the thickening of the muscle layer and the increased collagen production in the LP typically observed during intestinal schistosomiasis, it was not possible to adequately dissociate the *S. mansoni*-infected ileum without affecting cell viability. To this end, IHC and microscopic cell counts were performed as a complementary technique to the above mentioned MPFC analysis, which enabled us to quantitate the different cell subsets of interest in the mouse ileum in both healthy and *S. mansoni*-infected conditions. Our flow cytometry results of the MNP subsets in the mouse MLNs were obtained through rare event analysis and were consistent over a larger sample size of 11 *S. mansoni*-infected mice and 10 wild-type mice. Moreover, we were able to show that our *S. mansoni*-infection model, in addition to the FMO method, functions as a reliable positive control method hereby establishing a conservative and accurate gating strategy to measure the MNP populations in mouse MLNs (Fig. S3A–P). Our results indicate a significant increase in absolute CD11c^{+} CX3CR1^{+} F4/80^{-} LP DC numbers. The upregulation of this subset in the intestinal LP is indicative of a potentially interesting role in the immune response against *S. mansoni*. Quantitative flow cytometric analysis of the MLNs equally demonstrated a significant increase in this particular DC subset during *S. mansoni*-induced inflammation, indicating that CD11c^{+} CX3CR1^{+} F4/80^{-} are involved in the immune response against trematodes. These flow cytometry experiments showed, however, no significant change in the F4/80^{+} CX3CR1^{+} MΦ subset in the MLNs, leading us to hypothesize that CX3CR1^{+} MΦ have a subsidiary role in the immune response against *S. mansoni*-induced inflammation.

Our next step was to investigate which DC or MΦ subsets in the LP and MLNs were involved in parasite antigen uptake and processing and whether there were any discernible differences in their response. All subsets (CD11c^{-} CX3CR1^{+} cells, CD11c^{+} CX3CR1^{+} DC-like

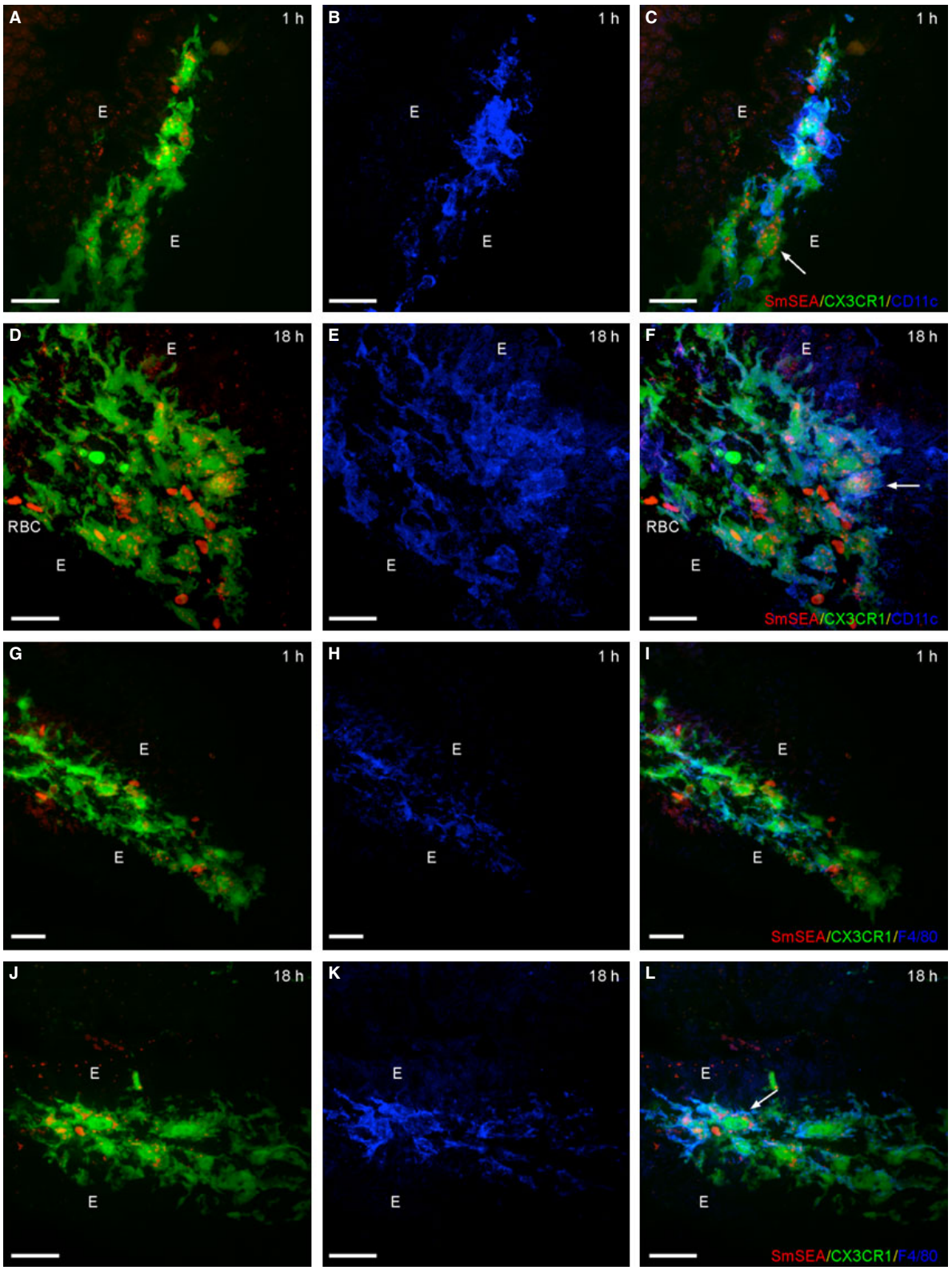

Figure 4 Uptake of SmSEA in the ileal lamina propria (LP). Cryosections of the ileum of CX3CR1$^{+/GFP}$ C57BL/6 mice immunostained for CD11c (A-F, in blue) or F4/80 (G- L, in blue) after *in vivo* SmSEA (in red) injections at different time points. CX3CR1^{+} cells (C, arrow), CD11c^{+} CX3CR1^{+} cells (F, arrow) and F4/80^{+} CX3CR1^{+} cells (L, arrow). E, epithelium; RBC, red blood cells. Scale bar: 20 μm.

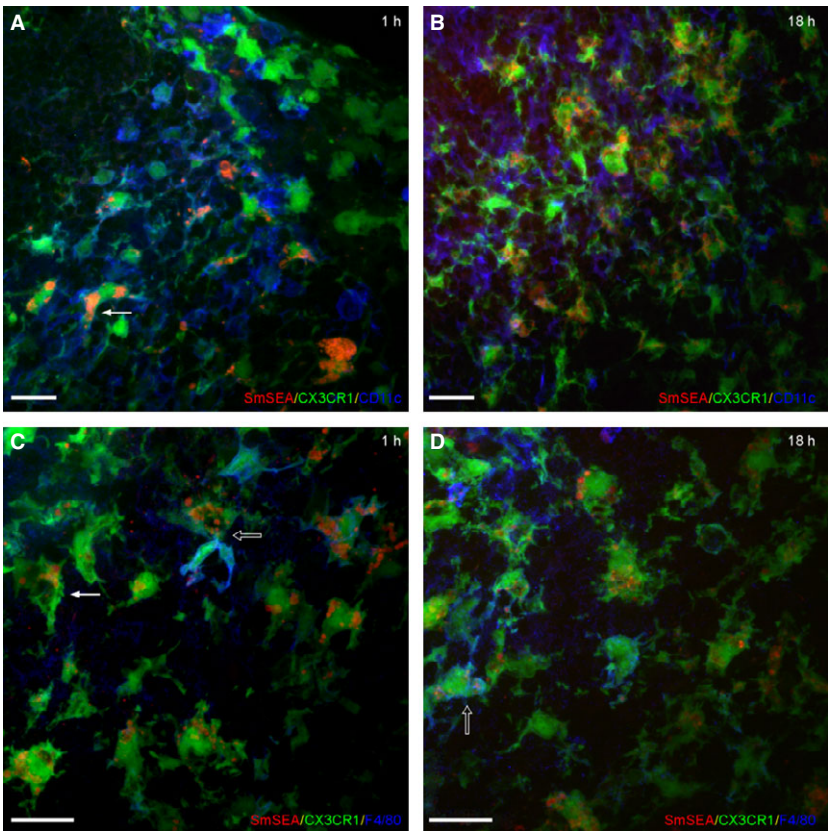

Figure 5 Uptake of SmSEA in the mesenteric lymph nodes (MLNs). Cryosections of the MLNs of CX3CR1$^{+/GFP}$ C57BL/6 mice immunostained for CD11c (A and B) or F4/80 (C and D) after *in vivo* SmSEA injections at different time points. CX3CR1^{+} cells (C, arrow), CD11c^{+} CX3CR1^{+} cells (A, arrow), and F4/80^{+} CX3CR1^{+} cells (C and D, open arrows). Scale bar: 20 μm.

cells, F4/80^{-} CX3CR1^{+} cells, F4/80^{+} CX3CR1^{-} cells and F4/80^{+} CX3CR1^{+} MΦ) actively engulfed either SmSWP or SmSEA antigens in both in the ileum and MLNs. Remarkably, mainly the CX3CR1-expressing subsets were involved in this antigen uptake and processing. The results clearly showed the presence of the MNP cell populations, *i.e.*, CD11c^{-} CX3CR1^{+} cells, CD11c^{+} CX3CR1^{+} DC-like cells, F4/80^{-} CX3CR1^{+} cells, F4/80^{+} CX3CR1^{-} cells, and F4/80^{+} CX3CR1^{+} MΦ, as immediate responses to the parasitic antigens. Following SmSWP or SmSEA uptake by the different cell types, the antigens were located within the lysosomes, indicating active antigen processing.

The present results showed the involvement of the different CX3CR1^{+} cell subsets and more specifically the CD11c^{+} CX3CR1^{+} F4/80^{-} DC subset in parasitic antigen uptake and processing. The rapid response observed after administration of the antigenic challenge indicated that these subsets participate in intestinal immune surveillance. This observation is indicative of possible migratory properties of these subsets. Our data show that the CX3CR1-expressing cell subsets respond immediately to schistosomal antigens both in the ileum and MLNs. At this point, we are unable to determine whether or not this event is due to a local effect, where the cells in the ileum and MLNs show a similar response to the antigens at the same time but in different anatomical locations or if there is active migration involved from the ileum to the MLNs after antigen exposure. This has to be the subject of extensive follow-up migration studies. Helminth therapy, especially with helminth-derived products, is regarded as a possible treatment for IBD and other inflammatory pathologies.[43] The beneficial effects of helminth treatment have been extensively described in animal studies and even clinical trials[44–46] in which different helminth species and derived products were employed. For example, infection with *S. mansoni* cercariae has been proven to produce protective effects in both trinitrobenzenesulfonic acid (TNBS)-induced colitis in rats and dextran sulphate sodium (DSS)-induced intestinal inflammation in mice.[47–49] Unlike the cercarial life stage, *S. mansoni* eggs and SmSEA did not ameliorate symptoms in a DSS-induced colitis mouse model,[49,50] although a protective effect of *S. mansoni* eggs in TNBS-induced intestinal inflammation in mice was reported in another study.[51] Helminth infection generally induces a Th2 or Treg biased immune response. Similar to our observations, Smith *et al.*[49] also found that the protective effect of *S. mansoni* worm infection against DSS-induced colitis was largely mediated by an enlarged population of F4/80^{+} MΦ.

The interplay between helminth products such as SmSWP and SmSEA and MNPs is an interesting target for the development of future therapies against intestinal inflammatory pathologies. This study highlight the importance of the CD11c$^+$ CX3CR1$^+$ F4/80$^-$ DC subset in the intestinal immune response, since an increase in this particular DC subset was observed in the ileal LP and in the MLNs during intestinal schistosomiasis. In addition, our *in vivo* experiments showed that the SmSWP and SmSEA antigens were rapidly and predominantly phagocytized by the CX3CR1-expressing MNP subsets in the LP and MLNs. Taken together, our results demonstrated the importance of the CX3CR1-expressing DC and MΦ cell subsets in intestinal immune surveillance and in the immune response against parasitic infection.

ACKNOWLEDGMENTS

The authors thank Dr. Gabriele Schramm from the Research Center Borstel in Germany for supplying the SmSEA, Danny Vindevogel for administrative assistance, Dominique De Rijck and Elien Theuns for technical assistance.

FUNDING

This study was supported by a TOP-BOF grant 22292 (to JPT and DA), a BOF-GOA project 28313 of the University of Antwerp (to ZB, BDW and JPT) and FWO-project grant G019314N (to RB and JPT) from the University of Antwerp, Belgium.

DISCLOSURE

All authors declare no conflicts of interest.

AUTHOR CONTRIBUTION

KA performed experiments, analyzed the data and wrote the largest part of the manuscript; RB designed the study, contributed funding, performed experiments and participated in data analysis and the writing of the manuscript; NC performed experiments, revised the manuscript critically and participated in data analysis; MH and SN participated in the SmSWP and SmSEA experiments; ZB, BDW, and DA revised the manuscript critically and provided essential research tools; LVN participated in the design of the study and critically revised the manuscript and JPT designed the study, critically revised the manuscript, provided essential reagents and research infrastructure and funded the study.

REFERENCES

1 Steinman RM. Decisions about dendritic cells: past, present, and future. *Annu Rev Immunol* 2012; **30**: 1–22.
2 Tezuka H, Ohteki T. Regulation of intestinal homeostasis by dendritic cells. *Immunol Rev* 2010; **234**: 247–58.
3 Xavier RJ, Podolsky DK. Unravelling the pathogenesis of inflammatory bowel disease. *Nature* 2007; **448**: 427–34.
4 Pavli P, Woodhams CE, Doe WF, Hume DA. Isolation and characterization of antigen-presenting dendritic cells from the mouse intestinal lamina propria. *Immunology* 1990; **70**: 40–7.
5 Helft J, Ginhoux F, Bogunovic M, Merad M. Origin and functional heterogeneity of non-lymphoid tissue dendritic cells in mice. *Immunol Rev* 2010; **234**: 55–75.
6 Bain CC, Scott CL, Uronen-Hansson H, Gudjonsson S, Jansson O, Grip O, Guilliams M, Malissen B *et al*. Resident and pro-inflammatory macrophages in the colon represent alternative context-dependent fates of the same Ly6Chi monocyte precursors. *Mucosal Immunol* 2013; **6**: 498–510.
7 Tamoutounour S, Henri S, Lelouard H, de Bovis B, de Haar C, van der Woude CJ, Woltman AM, Reyal Y *et al*. CD64 distinguishes macrophages from dendritic cells in the gut and reveals the Th1-inducing role of mesenteric lymph node macrophages during colitis. *Eur J Immunol* 2012; **42**: 3150–66.
8 Schulz O, Jaensson E, Persson EK, Liu X, Worbs T, Agace WW, Pabst O. Intestinal CD103$^+$, but not CX3CR1$^+$, antigen sampling cells migrate in lymph and serve classical dendritic cell functions. *J Exp Med* 2009; **206**: 3101–14.
9 Bogunovic M, Ginhoux F, Helft J, Shang L, Hashimoto D, Greter M, Liu K, Jakubzick C *et al*. Origin of the lamina propria dendritic cell network. *Immunity* 2009; **31**: 513–25.
10 Varol C, Vallon-Eberhard A, Elinav E, Aychek T, Shapira Y, Luche H, Fehling HJ, Hardt WD *et al*. Intestinal lamina propria dendritic cell subsets have different origin and functions. *Immunity* 2009; **31**: 502–12.
11 Coombes JL, Siddiqui KR, Arancibia-Carcamo CV, Hall J, Sun CM, Belkaid Y, Powrie F. A functionally specialized population of mucosal CD103$^+$ DCs induces Foxp3$^+$ regulatory T cells via a TGF-beta and retinoic acid-dependent mechanism. *J Exp Med* 2007; **204**: 1757–64.
12 Cerovic V, Houston SA, Scott CL, Aumeunier A, Yrlid U, Mowat AM, Milling SWF. Intestinal CD103(-) dendritic cells migrate in lymph and prime effector T cells. *Mucosal Immunol* 2013; **6**: 104–13.
13 Diehl GE, Longman RS, Zhang JX, Breart B, Galan C, Cuesta A, Schwab SR, Littman DR. Microbiota restricts trafficking of bacteria to mesenteric lymph nodes by CX3CR1(hi) cells. *Nature* 2013; **494**: 116–20.
14 Niess JH, Brand S, Gu X, Landsman L, Jung S, McCormick BA, Vyas JM, Boes M *et al*. CX3CR1-mediated dendritic cell access to the intestinal lumen and bacterial clearance. *Science* 2005; **307**: 254–8.
15 Chang SY, Song JH, Guleng B, Cotoner CA, Arihiro S, Zhao Y, Chiang HS, O'Keeffe M *et al*. Circulatory antigen processing by mucosal dendritic cells controls CD8(+) T cell activation. *Immunity* 2013; **38**: 153–65.
16 Cerovic V, Bain CC, Mowat AM, Milling SW. Intestinal macrophages and dendritic cells: what's the difference? *Trends Immunol* 2014; **35**: 270–7.
17 Alpaerts K, Buckinx R, Adriaensen D, Van Nassauw L, Timmermans JP. Identification and putative roles of distinct subtypes of intestinal dendritic cells in neuro-immune commu-

nication: what can be learned from other organ systems? *Anat Rec* 2015; **289**: 903–16.
18 Bogers J, Moreels T, De Man J, Vrolix G, Jacobs W, Pelckmans P, Van Marck E. *Schistosoma mansoni* infection causing diffuse enteric inflammation and damage of the enteric nervous system in the mouse small intestine. *Neurogastroenterol Motil* 2000; **12**: 431–40.
19 Wynn TA, Thompson RW, Cheever AW, Mentink-Kane MM. Immunop athogenesis of schistosomiasis. *Immunol Rev* 2004; **201**: 156–67.
20 Pearce EJ, MacDonald AS. The immunobiology of schistosomiasis. *Nat Rev Immunol* 2002; **2**: 499–511.
21 Everts B, Perona-Wright G, Smits HH, Hokke CH, van der Ham AJ, Fitzsimmons CM, Doenhoff MJ, van der Bosch J *et al*. Omega-1, a glycoprotein secreted by *Schistosoma mansoni* eggs, drives Th2 responses. *J Exp Med* 2009; **206**: 1673–80.
22 Everts B, Hussaarts L, Driessen NN, Meevissen MH, Schramm G, van der Ham AJ, van der Hoeven B, Scholzen T *et al*. Schistosome-derived omega-1 drives Th2 polarization by suppressing protein synthesis following internalization by the mannose receptor. *J Exp Med* 2012; **209**: 1753–67, S1.
23 McSorley HJ, Hewitson JP, Maizels RM. Immunomodulation by helminth parasites: defining mechanisms and mediators. *Int J Parasitol* 2013; **43**: 301–10.
24 Heylen M, Ruyssers NE, De Man JG, Timmermans JP, Pelckmans PA, Moreels TG, De Winter BY. Worm proteins of *Schistosoma mansoni* reduce the severity of experimental chronic colitis in mice by suppressing colonic proinflammatory immune responses. *PLoS ONE* 2014; **9**: e110002.
25 Heylen M, Ruyssers NE, Nullens S, Schramm G, Pelckmans PA, Moreels TG, De Man JG, De Winter BY. Treatment with egg antigens of *Schistosoma mansoni* ameliorates experimental colitis in mice through a colonic T-cell-dependent mechanism. *Inflamm Bowel Dis* 2015; **21**: 48–59.
26 Avula LR, Buckinx R, Alpaerts K, Costagliola A, Adriaensen D, Van Nassauw L, Timmermans JP. The effect of inflammation on the expression and distribution of the MAS-related gene receptors MrgE and MrgF in the murine ileum. *Histochem Cell Biol* 2011; **136**: 569–85.
27 Van Op den bosch J, Van Nassauw L, Van Marck E, Timmermans JP. Somatostatin modulates mast cell-induced responses in murine spinal neurons and satellite cells. *Am J Physiol Gastrointest Liver Physiol* 2009; **297**: G406–17.
28 Coombes JL, Powrie F. Dendritic cells in intestinal immune regulation. *Nat Rev Immunol* 2008; **8**: 435–46.
29 Yolles TK, Moore DV, Meleney HE. Post-cercarial development of *Schistosoma mansoni* in the rabbit and hamster after intraperitoneal and percutaneous infection. *J Parasitol* 1949; **35**: 276–94.
30 Jung S, Aliberti J, Graemmel P, Sunshine MJ, Kreutzberg GW, Sher A, Littman DR. Analysis of fractalkine receptor CX(3)CR1 function by targeted deletion and green fluorescent protein reporter gene insertion. *Mol Cell Biol* 2000; **20**: 4106–14.
31 Llewellyn-Smith IJ, Costa M, Furness JB. Light and electron microscopic immunocytochemistry of the same nerves from whole mount preparations. *J Histochem Cytochem* 1985; **33**: 857–66.
32 Ruyssers NE, De Winter BY, De Man JG, Loukas A, Pearson MS, Weinstock JV, Van den Bossche RM, Martinet W *et al*. Therapeutic potential of helminth soluble proteins in TNBS-induced colitis in mice. *Inflamm Bowel Dis* 2009; **15**: 491–500.
33 Lee JA, Spidlen J, Boyce K, Cai J, Crosbie N, Dalphin M, Furlong J, Gasparetto M *et al*. MIFlowCyt: the minimum information about a flow cytometry experiment. *Cytometry Part A*. 2008; **73**: 926–30.
34 Alvarez DF, Helm K, Degregori J, Roederer M, Majka S. Publishing flow cytometry data. *American J Physiol Lung Cell Mol Physiol* 2010; **298**: L127–30.
35 Hulspas R, O'Gorman MR, Wood BL, Gratama JW, Sutherland DR. Considerations for the control of background fluorescence in clinical flow cytometry. *Cytometry Part B, Clinical cytometry*. 2009; **76**: 355–64.
36 Tung JW, Heydari K, Tirouvanziam R, Sahaf B, Parks DR, Herzenberg LA, Herzenberg LA. Modern flow cytometry: a practical approach. *Clin Lab Med* 2007; **27**: 453–68, v.
37 Van Nassauw L, Brouns I, Adriaensen D, Burnstock G, Timmermans JP. Neurochemical identification of enteric neurons expressing P2X(3) receptors in the guinea-pig ileum. *Histochem Cell Biol* 2002; **118**: 193–203.
38 Ratcliffe EC, Wilson RA. The magnitude and kinetics of delayed-type hypersensitivity responses in mice vaccinated with irradiated cercariae of *Schistosoma mansoni*. *Parasitology* 1991; **103**(Pt 1): 65–75.
39 Schramm G, Gronow A, Knobloch J, Wippersteg V, Grevelding CG, Galle J, Fuller H, Stanley RG *et al*. IPSE/alpha-1: a major immunogenic component secreted from *Schistosoma mansoni* eggs. *Mol Biochem Parasitol* 2006; **147**: 9–19.
40 Merad M, Sathe P, Helft J, Miller J, Mortha A. The dendritic cell lineage: ontogeny and function of dendritic cells and their subsets in the steady state and the inflamed setting. *Annu Rev Immunol* 2013; **31**: 563–604.
41 Caulfield JP, Cianci CM. Human erythrocytes adhering to schistosomula of *Schistosoma mansoni* lyse and fail to transfer membrane components to the parasite. *J Cell Biol* 1985; **101**: 158–66.
42 Smith KA, Hochweller K, Hammerling GJ, Boon L, MacDonald AS, Maizels RM. Chronic helminth infection promotes immune regulation in vivo through dominance of CD11cloCD103- dendritic cells. *Journal of Immunology* 2011; **186**: 7098–109.
43 Heylen M, Ruyssers NE, Gielis EM, Vanhomwegen E, Pelckmans PA, Moreels TG, De Man JG, De Winter BY. Of worms, mice and man: an overview of experimental and clinical helminth-based therapy for inflammatory bowel disease. *Pharmacol Ther* 2014; **143**: 153–67.
44 Summers RW, Elliott DE, Urban JF Jr, Thompson R, Weinstock JV. Trichuris suis therapy in Crohn's disease. *Gut* 2005; **54**: 87–90.
45 Summers RW, Elliott DE, Urban JF Jr, Thompson RA, Weinstock JV. Trichuris suis therapy for active ulcerative colitis: a randomized controlled trial. *Gastroenterology* 2005; **128**: 825–32.
46 Sandborn WJ, Elliott DE, Weinstock J, Summers RW, Landry-Wheeler A, Silver N, Harnett MD, Hanauer SB. Randomised clinical trial: the safety and tolerability of Trichuris suis ova in patients with Crohn's disease. *Aliment Pharmacol Ther* 2013; **38**: 255–63.
47 Elliott DE, Urban JJ, Argo CK, Weinstock JV. Does the failure to acquire helminthic parasites predispose to

Crohn's disease? *FASEB J* 2000; **14**: 1848–55.
48 Moreels TG, Nieuwendijk RJ, De Man JG, De Winter BY, Herman AG, Van Marck EA, Pelckmans PA. Concurrent infection with *Schistosoma mansoni* attenuates inflammation induced changes in colonic morphology, cytokine levels, and smooth muscle contractility of trinitrobenzene sulphonic acid induced colitis in rats. *Gut* 2004; **53**: 99–107.
49 Smith P, Mangan NE, Walsh CM, Fallon RE, McKenzie AN, van Rooijen N, Fallon PG. Infection with a helminth parasite prevents experimental colitis via a macrophage-mediated mechanism. *Journal of Immunology.* 2007; **178**: 4557–66.
50 Bodammer P, Waitz G, Loebermann M, Holtfreter MC, Maletzki C, Krueger MR, Nizze H, Emmrich J *et al. Schistosoma mansoni* infection but not egg antigen promotes recovery from colitis in outbred NMRI mice. *Dig Dis Sci* 2011; **56**: 70–8.
51 Elliott DE, Li J, Blum A, Metwali A, Qadir K, Urban JF Jr, Weinstock JV. Exposure to schistosome eggs protects mice from TNBS-induced colitis. *Am J Physiol Gastrointest Liver Physiol* 2003; **284**: G385–91.

SUPPORTING INFORMATION

Additional supporting information may be found in the online version of this article at the publisher's web site:

Figure S1. Gating strategy and flow cytometric analysis of the mononuclear phagocytes (MNPs) in the ileal lamina propria (LP).

Figure S2. Gating strategy used for the subtyping of the different mononuclear phagocyte (MNP) subsets in the mesenteric lymph nodes (MLNs) of the mouse.

Figure S3. Flow cytometric analysis of the mononuclear phagocytes (MNPs) in the mesenteric lymph nodes (MLNs) under control conditions and during intestinal schistosomiasis.

Figure S4. Flow cytometric quantitation of the mononuclear phagocytes (MNPs) in the mesenteric lymph nodes (MLNs) under control conditions and during intestinal schistosomiasis.

Figure S5. Lysosomal localization of the SmSWP and SmSEA after phagocytosis.

Figure S6. Isotype control of the immunohistochemical analysis of the SmSWP and SmSEA- treated tissues.

Figure S7. Representative overview of the anatomical distribution of the immune cells involved in schistosomal antigen uptake.

Table S1. Primary antibodies (including their manufacturer and catalog number) used in the multiparametric flow cytometry experiments.

Table S2. Primary, secondary and tertiary antibodies (including dilution, manufacturers and catalog number) used in the immunohistochemistry experiments. All secondary antibodies are from Jackson Immunoresearch Laboratories Inc., West Grove, PA, USA.